

Interplay Between Optimal Selection Scheme, Selection Criterion, and Discrete Rate Adaptation in Opportunistic Wireless Systems

Neelesh B. Mehta, *Senior Member, IEEE*, Rajat Talak, *Student Member, IEEE*, and Ananda T. Suresh

Abstract—An opportunistic, rate-adaptive system exploits multi-user diversity by selecting the best node, which has the highest channel power gain, and adapting the data rate to selected node's channel gain. Since channel knowledge is local to a node, we propose using a distributed, low-feedback timer backoff scheme to select the best node. It uses a mapping that maps the channel gain, or, in general, a real-valued metric, to a timer value. The mapping is such that timers of nodes with higher metrics expire earlier. Our goal is to maximize the system throughput when rate adaptation is discrete, as is the case in practice. To improve throughput, we use a pragmatic selection policy, in which even a node other than the best node can be selected. We derive several novel, insightful results about the optimal mapping and develop an algorithm to compute it. These results bring out the inter-relationship between the discrete rate adaptation rule, optimal mapping, and selection policy. We also extensively benchmark the performance of the optimal mapping with several timer and opportunistic multiple access schemes considered in the literature, and demonstrate that the developed scheme is effective in many regimes of interest.

Index Terms—Cross-layer design, distributed selection, discrete rate adaptation, adaptive modulation and coding, timer scheme, fading channels, multiple access, collision, net throughput.

I. INTRODUCTION

CURRENT and next generation wireless systems achieve high downlink spectral efficiencies by exploiting multi-user diversity and rate adaptation [1], [2]. The base station or access point, which we henceforth refer to as the *sink*, selects the node to which it can transmit at the highest data rate. This has also been referred to as opportunistic selection in the literature [3]. Selection is also relevant to relay-based cooperative communications systems, which exploit spatial diversity by selecting a relay to forward data from the source to the destination [4]–[7].

A critical step in these systems is the selection of the node that can receive at the highest data rate. In the commonly used

contention-free polling scheme [1], each node sequentially feeds back to the sink the rate at which it can receive data; the sink then transmits to the best node with the highest rate. However, for such a scheme, the time required to find the best node increases linearly in the number of nodes, which reduces the fraction of time available for data transmission and lowers the net system throughput. Further, it impairs the ability of the system to handle time-varying channels.

Several multiple access-based algorithms have been proposed in the literature to address this problem [4], [8]–[10]. In the popular timer backoff scheme [4], [8], [11], [12], each node sets its timer as a function of its channel gain and transmits a small timer packet when its timer expires. The channel-gain-to-timer mapping is a monotone non-increasing function, which ensures that the timer of the best node always expires first. Therefore, the sink simply selects the node whose timer packet it receives first, and transmits to it at an appropriate rate. Thus, the timer scheme also effectively acts as a channel quality feedback scheme.

The timer scheme is practically appealing because it requires minimal feedback from the sink. It can also be easily adapted to implement proportional fairness – each node set its timer as a function of the ratio of its channel gain to its mean channel gain [3], [13]. Other notions of fairness and quality of service can also be incorporated in a similar manner [5], [14].

In practice, for the best node to get selected, not only must its timer expire, but also no other node's timer must expire within a vulnerability window of duration Δ after the expiry of the timer of the best node [15]. Otherwise, a collision occurs and the system fails to select the best node. The system-specific parameter Δ accounts for the maximum propagation and detection delay, time synchronization errors, and the node's timer packet duration [4]. Thus, selection takes up resources such as time, and the best node may sometimes not be selected. These depend on the timer mapping used, and ultimately affect the throughput achieved by the system.

A. Model Overview and Contributions

In this paper, we characterize the structure of an optimal timer mapping that maximizes the downlink throughput of a system that consists of k nodes and a sink. Each node maintains a local metric, which is a function of its downlink channel gain. The higher the channel gain, the higher the metric. All the nodes set their timers as a function of their

Manuscript received July 17, 2012; revised December 18, 2012 and February 11, 2013. The editor coordinating the review of this paper and approving it for publication was H. Dai.

Preliminary results in the paper were presented at the National Conf. on Communications (NCC), Chennai, India, Jan. 2010.

N. B. Mehta and R. Talak are with the Dept. of Electrical Communication Eng. (ECE), Indian Institute of Science (IISc), Bangalore, India (e-mail: nbmehta@ece.iisc.ernet.in, rajatalak@gmail.com).

A. T. Suresh is with the Dept. of Electrical and Computer Eng., Univ. of California, San Diego, CA, USA (e-mail: asuresh@ucsd.edu).

This research was partly supported by DST, India, and EPSRC, UK under the auspices of the India-UK Advanced Technology Center (IU-ATC).

Digital Object Identifier 10.1109/TCOMM.2013.043013.120517

metrics. Thus, timers of nodes with higher metrics expire earlier. When its timer expires, a node transmits a timer packet to the sink on the uplink. The sink then transmits data at an appropriate rate to the selected node on the downlink. There are two important facets to the model considered in this paper:

- 1) *Pragmatic selection*: The sink waits for the first timer packet that it can reliably detect – even if collisions precede it – and selects the node that transmitted it. This is different from best node selection, in which an outage is declared if the best node is not selected.
- 2) *Discrete rate adaptation*: The sink can transmit to the selected node using only one out of M pre-specified rates, as is the case in practical wireless systems. This has implications on the design of the timer scheme. For example, even though the channel gain of the best node exceeds that of the second best node or, in general, the l^{th} best node, these nodes may support the same rate. In such a case, it does not matter which node among these nodes gets selected. This issue does not arise in the idealized Shannon capacity-based continuous rate adaptation models considered in [4], [8], [16], [17].

We make the following specific contributions in this paper:

- We characterize an optimal timer mapping that maximizes the average data rate given a maximum selection duration T_{\max} , vulnerability window Δ , and a rate adaptation policy. Given its optimality, the result serves as a useful benchmark for other selection schemes.
- Determining the optimal scheme turns out to be computationally intensive, and is a key challenge that this paper addresses. We develop several results about the structure of the optimal timer mapping, which culminate in an algorithm to compute the optimal mapping.
- We derive an expression for the average data rate achieved by the optimal mapping. An approximate expression is also derived to efficiently compute it.
- To quantify the joint impact of the selection policy and selection scheme, we benchmark the performance of the proposed optimal scheme with several opportunistic approaches proposed in the literature [4], [17]–[19]. We observe that the extent of the performance gains over these benchmark schemes depends on the number of nodes and the data transmission duration.
- In addition to determining the optimal mapping for a given T_{\max} , we also optimize T_{\max} to maximize the net system throughput.

B. Related Literature and Comparisons

Several timer mappings have been proposed in the literature. In the inverse metric mapping [4], a node with metric μ sets its timer as $\frac{c}{\mu}$, where $c > 0$ is a constant. Instead, in the linear piece-wise continuous mapping [8], the timer is set to T_{\max} if $\mu \leq \zeta_l$, as 0 if $\mu \geq \zeta_u$, and as $\frac{\zeta_u - \mu}{\zeta_u - \zeta_l} T_{\max}$ if $\zeta_l < \mu < \zeta_u$, where ζ_l and ζ_u are constants. In [11], the timer is set as $(1 - \mu)^{\frac{1}{1+\kappa}}$, where $\kappa > 0$ is a constant and μ is normalized to lie in between 0 and 1. The scheme proposed in [17] can also be interpreted as a discrete timer mapping. In it, the range of values that the metric can take is divided into Z equi-probable intervals. Nodes set their timers depending

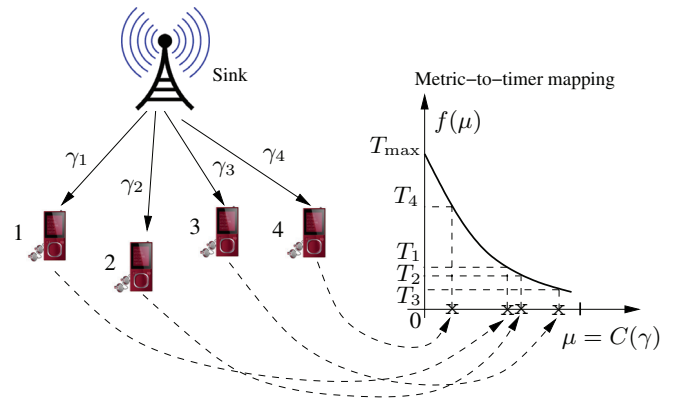


Fig. 1. A system consisting of a base station and k nodes. Each node j sets its timer depending on its signal-to-noise ratio, γ_j , or, equivalently, its metric μ_j .

upon which interval their metrics lie in, and timers of nodes with larger metrics expire earlier. In the timer mapping used in [18], [20], the probability of a transmission in the next slot, given that no node transmitted in any of the earlier slots, is kept constant. However, unlike our approach, all the above mappings are ad hoc and are not designed to maximize the system throughput.

An optimal timer mapping that maximizes the probability of selecting the best node given a maximum selection duration T_{\max} was derived in [19]. However, focusing only on selecting the best node is pessimistic because the sink may fail to select it and yet be able to transmit at a non-zero data rate to the l^{th} best node ($l \geq 2$). A different multiple access-based selection approach was pursued in [16]. In it, time is divided into multiple slots. Each node transmits in a slot with probability p if its channel gain exceeds a pre-specified threshold η . Among the nodes whose transmissions did not collide, one is selected randomly. However, unlike our approach, all nodes whose channel gains exceed η are treated equally.

The paper is organized as follows. Section II describes the system model. The optimal timer scheme and its performance are derived in Section III. Simulation results and conclusions follow in Sec. IV and Sec. V, respectively. Mathematical proofs are relegated to the Appendix.

II. SYSTEM MODEL

Consider a system with k nodes and a sink, as shown in Figure 1. The downlink channels from the sink to the nodes are assumed to undergo flat fading and are independent and identically distributed (i.i.d.). The independence assumption is justified because the nodes are geographically separated. The identicalness assumption makes the problem tractable, and is commonly made in the related literature [4], [8]–[10], [19]. The channel gains are assumed to not change over the duration of selection and data transmission. Let γ_j denote the signal-to-noise ratio (SNR) of the downlink channel from the sink to node j . It is known only to node j but not to the sink or the other nodes. Sorting the gains in descending order, we get $\gamma_{(1)} > \gamma_{(2)} > \dots > \gamma_{(k)}$, where (l) , as per order statistics notation [21], denotes the index of the node with the l^{th} largest gain.

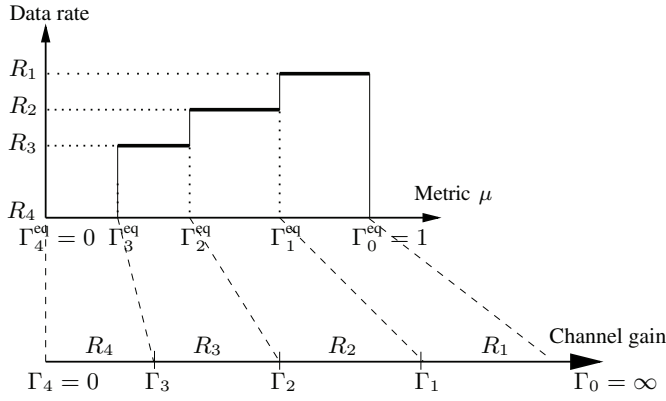


Fig. 2. Illustration of discrete rate adaptation as a function of the metric for $M = 4$ rates ($R_1 > R_2 > R_3 > R_4 = 0$).

Our goal is to come up with a general design that holds for any given probability distribution of the SNRs. To this end, we define the metric of node j as

$$\mu_j = C(\gamma_j), \quad (1)$$

where $C(\cdot)$ is the cumulative distribution function (CDF) of γ_j . It is assumed to be continuous, as is the case for several wireless channel models, and known at all the nodes along with k [9], [10], [19]. A key outcome of (1) is that μ_j is a random variable (RV) that is uniformly distributed in the interval $[0, 1)$ [22]. And, the monotonicity of C preserves order, i.e., the node with the l^{th} largest SNR is also the node with the l^{th} largest metric.

A. Discrete Rate Adaptation Rule

Let $0 = R_M < R_{M-1} < \dots < R_1$ denote the set of M rates available to the system. Say the sink selects node j . It will transmit to it at a rate R_i if $\gamma_j \in [\Gamma_i, \Gamma_{i-1})$ [23]. Here, $0 = \Gamma_M < \Gamma_{M-1} < \dots < \Gamma_0 = \infty$ are called the *adaptation thresholds*. Equivalently, let $\psi(\mu_j)$ denote the rate assigned to node j with metric μ_j . It equals R_i if $\mu_j \in [\Gamma_i^{\text{eq}}, \Gamma_{i-1}^{\text{eq}})$, where $\Gamma_i^{\text{eq}} = C(\Gamma_i)$. We shall refer to $\Gamma_1^{\text{eq}}, \dots, \Gamma_M^{\text{eq}}$ as the *normalized adaptation thresholds*. Formally,

$$\psi(\mu_j) = R_i, \quad \text{if } \Gamma_i^{\text{eq}} \leq \mu_j < \Gamma_{i-1}^{\text{eq}}, \quad \text{where } 1 \leq i \leq M. \quad (2)$$

This rule is illustrated in Fig. 2.

The discrete rate adaptation rule in terms of metrics is best understood by the following example. From [23], for a Q -ary QAM constellation, the rate is $\log_2 Q$ bits/symbol and the bit error rate (BER) as a function of the SNR γ is

$$\text{BER} \approx 0.2 \exp\left(-\frac{1.5\gamma}{Q-1}\right), \quad Q \geq 4. \quad (3)$$

Rearranging terms and taking logarithms on both sides of (3), we get $\Gamma_i = \frac{(2^{R_i-1})}{1.5} \log_e\left(\frac{1}{5P_b}\right)$, where P_b is the target BER. For Rayleigh fading, the CDF is $C(\gamma) = 1 - \exp(-\gamma/\bar{\gamma})$, for $\gamma \geq 0$, where $\bar{\gamma}$ is the average SNR. Therefore, $\mu = 1 - \exp(-\gamma/\bar{\gamma})$. It can then be shown that $\Gamma_i^{\text{eq}} = 1 - (5P_b)^{\left(\frac{2^{R_i-1}}{1.5\bar{\gamma}}\right)}$. The above framework applies equally well to other constellations or coded modulation schemes [23], [24]. A similar exponential relationship between the rates

and the thresholds also arises when one uses the coding loss model [24]. In this case, we have $\Gamma_i = \frac{2^{R_i-1}}{\zeta}$, where $0 < \zeta < 1$ is the coding loss of a practical code.

B. Timer-based Selection Scheme and Selection Policy

We now describe the timer-based scheme that is used to select a node. Node j sets its timer T_j as a function of its metric μ_j as $T_j = f(\mu_j)$, as shown in Fig. 1. Here, f is a monotone non-increasing (MNI) function and is called the *metric-to-timer mapping*. It transmits a small packet to the sink on the uplink when its timer expires, which happens if $T_j \leq T_{\text{max}}$, where T_{max} is the time allocated for selection. The timer packet contains the node's identity to enable the sink to identify the node; it contains no other information. We say that $T_j = T_{\text{max}}^+$ when the timer of node j does not expire. As mentioned, if two timers expire within a duration Δ of each other, their timer packets collide and cannot be decoded by the sink [4], [15].

The sink waits for the first timer packet that it can reliably detect and selects the node that transmitted it. For this, the selected node's timer packet must not overlap in time with the timer packet of any other node. For example, the best node gets selected if no other node's timer expires within a window Δ of its timer's expiry. However, the third best node may get selected in case the timers of the best and second best nodes collided at least Δ s earlier. As mentioned, selecting a node other than the best node is better than declaring outage when the best node is not selected. After selection, the sink transmits data of duration T_d to the selected node on the downlink. However, if no node transmits successfully by T_{max} , the sink declares outage, in which case no data is transmitted. This process of selection followed by data transmission is repeated once in every coherence interval. Note that the nodes are not required to overhear each other's transmissions, which avoids the hidden node problem.

III. OPTIMAL TIMER MAPPING CHARACTERIZATION

We shall use the following notation henceforth. $\mathbf{E}[X]$ denotes the expectation of the RV X , and $\mathbf{E}[X|A]$ denotes the conditional expectation given A . The optimal value of a parameter x is denoted by x^* . Further, the summation $\sum_{i=a}^b$ is identically equal to zero if $b < a$.

A. Overview of Results

We now derive a sequence of results about the structure of the optimal timer mapping that maximizes the average data rate with the pragmatic selection policy given the number of nodes k , rate adaptation rule, vulnerability window Δ , and maximum selection duration T_{max} . The results are presented in the following order:

- 1) We first show in Result 1 an intuitive result that only the timers of nodes that support a non-zero data rate may expire in the optimal timer mapping.
- 2) We then show in Result 2 that the optimal mapping that maximizes the average data rate is an MNI staircase mapping, which is shown in Figure 3. In it, the timer can expire only at times $0, \Delta, \dots, \text{or } N\Delta$, or not at all.

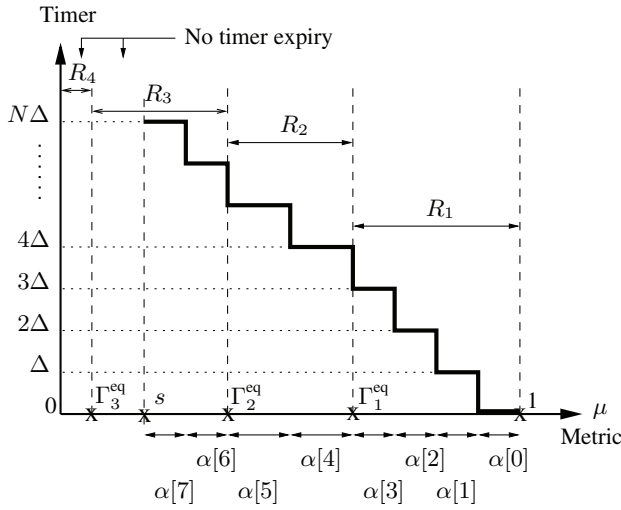


Fig. 3. Illustration of the optimal timer mapping for $N = 7$ and $M = 4$ rates. The figure shows that $r_1 = 4$ equal length intervals occupy the entire interval $[\Gamma_1^{\text{eq}}, 1]$ in which the data rate is R_1 . Similarly, $r_2 = 2$ equal length intervals occupy the interval $[\Gamma_2^{\text{eq}}, \Gamma_1^{\text{eq}}]$ in which the data rate is R_2 . And, $r_3 = 2$ equal length intervals occupy the interval $[s, \Gamma_2^{\text{eq}}]$, where $\Gamma_3^{\text{eq}} \leq s < \Gamma_2^{\text{eq}}$. The timers of all nodes whose metrics lie in $[0, s)$ do not expire.

This reduces the problem of finding the optimal mapping from the space of all MNI functions to the space of MNI staircase functions, which are completely characterized by $N+1$ parameters, which we call interval lengths. The reason for this terminology shall become clear later.

- 3) Using Result 2, we then derive in Result 3 an expression for the average data rate achieved by a staircase mapping with pragmatic selection. We also derive in Result 4 an alternate recursive expression for the average data rate, which leads to a computationally efficient approximation for evaluating it.
- 4) Thereafter, using all the above results, in Result 5 we establish a connection between the interval lengths and the $M+1$ adaptation thresholds, which reduces the search for the optimal mapping to finding at most M positive integers that sum up to $N+1$ and a real number.
- 5) The above five results together culminate in the algorithm in Sec. III-C to compute the optimal timer mapping.

B. Structure of Optimal Timer Mapping

Result 1: There exists an optimal timer mapping such that timers of all nodes whose metrics are less than Γ_{M-1}^{eq} do not expire by time T_{max} .

Proof: The proof is relegated to Appendix A. ■

The above result confirms the intuition that if a node's channel condition is so poor that it cannot transmit with a non-zero rate, then it need not participate in the selection scheme. We now prove that the range of the optimal mapping that maximizes the average data rate with pragmatic selection is discrete and bounded.

Result 2: There exists an optimal timer mapping entirely defined by $N+1$ positive real numbers $\alpha[0], \dots, \alpha[N]$ such that a node whose metric lies in the interval $[1 - \alpha[0], 1)$ sets its timer to expire at 0; a node whose metric lies in the

interval $[1 - \alpha[1] - \alpha[2], 1 - \alpha[1])$ sets its timer to expire at Δ , and so on. In general, the timer of a node whose metric lies in the interval $[1 - \sum_{j=0}^i \alpha[j], 1 - \sum_{j=0}^{i-1} \alpha[j])$ expires at $i\Delta$. The timer of a node whose metric lies in the interval $[0, 1 - \sum_{j=0}^N \alpha[j])$ does not expire.

Proof: The proof is given in Appendix B. ■

Thus, the timers can only expire at the time instants $0, \Delta, \dots, N\Delta$. This result is analogous to a well-known result in multiple access control protocol design, which shows that slotted Aloha, which allows transmissions only at discrete time instants, achieves a higher throughput than unslotted Aloha [25]. We shall refer to such a mapping as a *discrete timer mapping*. It is illustrated in Fig. 3. Notice that it resembles a staircase, in which each stair has a height of Δ . Therefore, we shall also call it a *staircase mapping*. We shall refer to the interval $[1 - \sum_{j=0}^i \alpha[j], 1 - \sum_{j=0}^{i-1} \alpha[j])$ as the i^{th} interval and $\alpha[i]$ as the length of the i^{th} interval, for $0 \leq i \leq N$. Further, we shall say that a node *lies in an interval* when its metric belongs to that interval. For ease of exposition, we shall refer to the interval $[0, 1 - \sum_{i=0}^N \alpha[i])$ as the $(N+1)^{\text{th}}$ interval. Let $\alpha[N+1] \triangleq 1 - \sum_{i=0}^N \alpha[i]$.

1) *Analysis of Average Data Rate:* We now express the average data rate in terms of the $N+1$ interval lengths $\alpha[0], \dots, \alpha[N]$. First note that when a node that lies in the j^{th} interval is selected, the downlink data rate is equal to $\psi(1 - \sum_{i=0}^j \alpha[i])$. This is because the sink will transmit at a rate that can be reliably decoded by the selected node, and all it knows is that the metric of the selected node lies in the interval $[1 - \sum_{i=0}^j \alpha[i], 1 - \sum_{i=0}^{j-1} \alpha[i])$.

For a given realization of metrics, let x_0 denote the number of nodes whose metrics lie in the 0^{th} interval $[1 - \alpha[0], 1)$, let x_1 denote the number of nodes whose metrics lie in the 1^{st} interval $[1 - \alpha[0] - \alpha[1], 1 - \alpha[0])$, and in general, let x_l be the number of nodes whose metrics lie in the l^{th} interval $[1 - \sum_{j=0}^l \alpha[j], 1 - \sum_{j=0}^{l-1} \alpha[j])$. To arrive at a compact expression for the average data rate, we first define a *selection location function*, $S(\mathbf{x})$, for the vector $\mathbf{x} = (x_0, x_1, \dots, x_N) \in \mathbb{Z}^{N+1}$, as follows:

$$S(\mathbf{x}) \triangleq \begin{cases} l, & \text{if } x_l = 1 \text{ and } x_j \neq 1, \text{ for all } j < l, \\ N+1, & \text{otherwise.} \end{cases} \quad (4)$$

The selection location function is useful for tracking whether and where the successful transmission occurs for the following reasons. Recall that a node that lies in the l^{th} interval gets selected if and only if no success occurs in the intervals $0, \dots, l-1$ that precede the l^{th} interval and only that node lies in the l^{th} interval. This is equivalent to the condition that $x_j \neq 1$, for $0 \leq j \leq l-1$, and $x_l = 1$. Therefore, when this is the case, we get $S(\mathbf{x}) = l$. Furthermore, when all the nodes collided or no timers expired by time T_{max} , no success occurs. In this case $x_j \neq 1$, for all $0 \leq j \leq N$, and we get $S(\mathbf{x}) = N+1$. In essence, the selection location function mathematically defines pragmatic selection for the timer scheme.

We now derive an expression for the average data rate, which is denoted by $\bar{R}_{N,k}$.

Result 3: The average data rate of the discrete timer map-

ping is given by

$$\begin{aligned} \bar{R}_{N,k} = & \sum_{\substack{\mathbf{x}=(x_0,\dots,x_N) \\ x_j \geq 0, \sum_{j=0}^N x_j \leq k}} \binom{k}{x_0, \dots, x_N} \left[\prod_{i=0}^N (\alpha[i])^{x_i} \right] \\ & \times \left(1 - \sum_{l=0}^N \alpha[l] \right)^{k - \sum_{j=0}^N x_j} \psi \left(1 - \sum_{j=0}^{\mathcal{S}(\mathbf{x})} \alpha[j] \right), \quad (5) \end{aligned}$$

where $\binom{k}{x_0, \dots, x_N}$ denotes the multinomial expression and $\sum_{\substack{\mathbf{x}=(x_0,\dots,x_N) \\ x_j \geq 0, \sum_{j=0}^N x_j \leq k}}$ denotes the summation over all $(N+1)$ -tuples that consist of positive integers whose sum is less than or equal to k .

Proof: The proof is given in Appendix C. ■

The result can be intuitively understood as follows. Depending on the realizations of the metrics of the k nodes, different numbers of nodes will lie in the $N+1$ intervals $\alpha[0], \dots, \alpha[N]$. The probability that this happens is given by a multinomial distribution, which gives rise to the $\binom{k}{x_0, \dots, x_N} \left[\prod_{i=0}^N (\alpha[i])^{x_i} \right] \left(1 - \sum_{l=0}^N \alpha[l] \right)^{k - \sum_{j=0}^N x_j}$ term in (5). The above result averages the data rates achieved by the various possible configurations for the numbers of nodes that lie in the $N+1$ intervals.

2) Simplifying the Computation of Average Data Rate:

Notice that computing the average data rate in (5) involves summing over many $(N+1)$ -tuples \mathbf{x} . We now show that the average data rate expression can be written in an alternate, recursive manner. This then leads to a computationally simpler and accurate approximation for it.

Result 4: The average data rate $\bar{R}_{N,k}$ of the discrete timer mapping is given by

$$\begin{aligned} \bar{R}_{N,k} = & k\alpha[0] (1 - \alpha[0])^{k-1} \psi(1 - \alpha[0]) + (1 - \alpha[0])^k \bar{R}'_{N-1,k} \\ & + \sum_{r=2}^k \binom{k}{r} \alpha[0]^r (1 - \alpha[0])^{k-r} \bar{R}'_{N-1,k-r}, \quad (6) \end{aligned}$$

where $\bar{R}'_{N-1,k-r}$ is the average data rate obtained when there are $k-r$ nodes, an $(N-1)$ -level timer with interval lengths given by $\frac{\alpha[1]}{1-\alpha[0]}, \dots, \frac{\alpha[N]}{1-\alpha[0]}$ is used, and the rate function given by $\psi'(x) \triangleq \psi((1 - \alpha[0])x)$. The initialization points for the above recursion are as follows:

$$\bar{R}_{0,k} = k\alpha[0] (1 - \alpha[0])^{k-1} \psi(1 - \alpha[0]), \quad (7)$$

$$\bar{R}_{N,1} = \sum_{j=0}^N \alpha[j] \psi \left(1 - \sum_{l=0}^j \alpha[l] \right). \quad (8)$$

Proof: The proof is relegated to Appendix D. ■

The above recursion arises because if an idle occurs in the first interval, then, conditioned on this event, we know that metrics of all the k nodes are uniformly distributed and i.i.d. in the interval $[0, 1 - \alpha[0]]$. Similarly, consider the case when $r \geq 2$ nodes collided in the first interval. Then, conditioned on this event, the metrics of the remaining $k-r$ nodes are uniformly distributed and i.i.d. in $[0, 1 - \alpha[0]]$. It is for this reason that the scaling factor of $1 - \alpha[0]$ appears in (6). Further,

given that r nodes transmit in the first interval, the average data rate is $\bar{R}'_{N-1,k-r}$, where $r = 0$ or $r \geq 2$.

Truncating the series in (6) yields the following computationally simpler approximation for evaluating $\bar{R}_{N,k}$:

$$\begin{aligned} \bar{R}_{N,k} \approx & k\alpha[0] (1 - \alpha[0])^{k-1} \psi(1 - \alpha[0]) + (1 - \alpha[0])^k \bar{R}'_{N-1,k} \\ & + \binom{k}{2} \alpha[0]^2 (1 - \alpha[0])^{k-2} \bar{R}'_{N-1,k-2}. \quad (9) \end{aligned}$$

This means that we neglect the possibility that more than two nodes collide in the zeroth interval. This approximation is tight for $\alpha[0] \ll 1$.

3) *Average Data Rate Optimization Problem:* With the help of the results and notation developed thus far, the throughput optimization problem can now be compactly stated as follows:

$$\begin{aligned} & \max_{\alpha[0], \dots, \alpha[N]} \bar{R}_{N,k} \\ & \text{subject to } \alpha[i] \geq 0, \text{ for } 0 \leq i \leq N, \quad (10) \end{aligned}$$

$$\sum_{i=0}^N \alpha[i] \leq 1 - \Gamma_{M-1}^{\text{eq}}. \quad (11)$$

Note that the constraint in (11) follows from Result 1 because it shows that the timers of the nodes that lie in $[0, \Gamma_{M-1}^{\text{eq}})$, in which the rate is 0, do not expire.

To solve the above optimization problem we assume that the normalized thresholds lie at the boundaries of the timer intervals. The effect of this assumption will be evaluated in Sec. IV. Therefore, let r_1 intervals lie in the interval $[\Gamma_1^{\text{eq}}, 1)$, r_2 intervals lie in $[\Gamma_2^{\text{eq}}, \Gamma_1^{\text{eq}})$, and so on, up to r_m intervals lie in $[\Gamma_m^{\text{eq}}, \Gamma_{m-1}^{\text{eq}})$. Here, m is an integer such that $\sum_{i=1}^m r_i = N+1$. From (11), we know that $1 - \Gamma_M^{\text{eq}} > \sum_{i=0}^N \alpha^*[i] = \alpha^*[N+1]$. This implies that $m \leq M-1$.

Result 5: In the optimal mapping, the first r_1 intervals have the same length, the next r_2 intervals have the same length, and so on:

$$\begin{aligned} \alpha^*[0] = \dots = \alpha^*[r_1 - 1] &= \frac{1 - \Gamma_1^{\text{eq}}}{r_1}, \\ \alpha^*[r_1] = \dots = \alpha^*[r_1 + r_2 - 1] &= \frac{\Gamma_1^{\text{eq}} - \Gamma_2^{\text{eq}}}{r_2}, \\ & \vdots \\ \alpha^* \left[\sum_{i=1}^{m-2} r_i \right] = \dots = \alpha^* \left[\sum_{i=1}^{m-1} r_i - 1 \right] &= \frac{\Gamma_{m-2}^{\text{eq}} - \Gamma_{m-1}^{\text{eq}}}{r_{m-1}}, \\ \alpha^* \left[\sum_{i=1}^{m-1} r_i \right] = \dots = \alpha^*[N] &= \frac{s}{r_m}, \quad (12) \end{aligned}$$

where $0 < s < \Gamma_{m-1}^{\text{eq}} - \Gamma_m^{\text{eq}}$ is a real number.

Proof: The proof is relegated to Appendix E. ■

The above result brings out the inter-relationship between the optimal timer mapping and the discrete rate adaptation rule. It arises due to the symmetry of the average data rate expression in (5). Figure 3 illustrates the final structure of the optimal timer mapping.

C. Algorithm to Compute Optimal Mapping's Parameters

Given Result 5, finding the optimal mapping that maximizes $\bar{R}_{N,k}$ has reduced to finding an integer $m \in \{1, \dots, M-1\}$,

positive integers r_1, \dots, r_m , such that $\sum_{i=1}^m r_i = N + 1$, and a real number $s \in (0, \Gamma_{m-1}^{\text{eq}} - \Gamma_m^{\text{eq}}]$. Recall that k is the number of nodes, M is the number of rates, and N is the number of timer levels. We now present an iterative algorithm to compute these parameters, and, hence, the optimal mapping. Its pseudo-code is given in Fig. 4.

```

Data:  $N, k$ , and resolution  $\delta$ 
Result:  $\alpha^*[i], \forall 0 \leq i \leq N$ , and  $\bar{R}_{N,k}^*$ 
begin
   $s \leftarrow 1$  and  $\bar{R}_{N,k}^* \leftarrow 0$ ;
  while  $s \geq \Gamma_{M-1}^{\text{eq}} + \delta$  do
     $s \leftarrow s - \delta$ ;
    Find  $m$  such that (s.t.)  $\Gamma_m^{\text{eq}} < s \leq \Gamma_{m-1}^{\text{eq}}$ 
    Let  $\mathcal{C}_m \leftarrow$  Set of all integer  $m$ -tuples
     $\{r_1, \dots, r_m\}$  s.t.  $r_j > 0, \forall j \leq m$ , and
     $\sum_{j=1}^m r_j = N + 1$ ;
    while  $\mathcal{C}_m \neq \phi$  (null set) do
      Pick a tuple  $\omega \in \mathcal{C}_m$ ;
      Given  $\omega$ : Compute  $\alpha[i], \forall 0 \leq i \leq N$ 
      (from (12) of Result 5) and  $\bar{R}_{N,k}$  (from (5));
      if  $\bar{R}_{N,k}^* < \bar{R}_{N,k}$  then
         $\bar{R}_{N,k}^* \leftarrow \bar{R}_{N,k}; \alpha^*[i] \leftarrow \alpha[i],$ 
         $\forall 0 \leq i \leq N$ ;
      end
       $\mathcal{C}_m \leftarrow \mathcal{C}_m \setminus \{\omega\}$ ;
    end
  end
end

```

Fig. 4. Algorithm to compute optimal timer scheme's parameters based on Results 1, 2, ..., 5.

Briefly, the algorithm works as follows. It starts with $s = 1 - \delta$, which implies that $m = 1$ initially. It then reduces s in steps of δ in each iteration. Given s , the optimal values of r_1, \dots, r_m that maximize the average data rate are determined by searching over the positive integer m -tuples that satisfy the constraint $\sum_{i=1}^m r_i = N + 1$. Given r_1, \dots, r_m , the average data rate can be directly determined from (5) or its simpler variant in (9). Once s falls below Γ_1^{eq} , m increases to 2, and so on. The algorithm clearly terminates since $s > 0$. It yields the optimal mapping, in which each optimal interval length is computed to an accuracy of at least δ .

IV. NUMERICAL RESULTS AND PERFORMANCE BENCHMARKING

We now numerically study the properties of the proposed optimal timer scheme and verify our analytical results using Monte Carlo simulations. For this purpose, we use the discrete rate adaptation used by the Long Term Evolution (LTE) cellular communications standard. In it, $M = 16$ possible rates can be fed back by a node [26, Table 7.2.3-1]. The spectral efficiencies of these rates range from $R_{16} = 0$ to $R_1 = 5.55$ bits/symbol. The equivalent thresholds $\Gamma_0^{\text{eq}}, \dots, \Gamma_{16}^{\text{eq}}$ are determined by the aforementioned coding loss model with $\zeta = 0.398$ [24].

TABLE I
COMPARISON OF INTERVAL LENGTHS OF DIFFERENT TIMER MAPPINGS.
ONLY THE INTERVALS IN WHICH THE TIMERS EXPIRE ARE SHOWN

	Proposed timer		Max. success prob. timer [19]		Eq. intervals timer [17]		Fixed 90% tx. prob. timer [18]	
	2	3	2	3	2	3	—	—
N	2	3	2	3	2	3	—	—
k	10	100	10	100	10	100	10	100
$\alpha[0]$	0.010	0.010	0.047	0.004	0.333	0.250	0.0227	0.0021
$\alpha[1]$	0.025	0.008	0.060	0.005	0.333	0.250	0.0222	0.0021
$\alpha[2]$	0.076	0.008	0.089	0.006	0.333	0.250	0.0217	0.0021
$\alpha[3]$	-	0.008	-	0.010	-	0.250	0.0212	0.0021
$\alpha[4]$	-	-	-	-	-	-	0.0207	0.0021
$\alpha[5]$	-	-	-	-	-	-	0.0202	0.0021
$\alpha[6]$	-	-	-	-	-	-	0.0198	0.0021

A. Comparison with Timer Schemes

Table I compares the optimal interval lengths, as obtained from the above algorithm, with the interval lengths of several other discrete timer mappings proposed in the literature [17]–[19]. This is done for different values of N and k . Notice that the optimal interval lengths decrease as k increases, and are different from those that maximize the probability of selecting the best node. Furthermore, in the equal (eq.) intervals timer mapping [17] and the fixed transmission (tx.) probability mapping [18], there is no region in the $[0, 1)$ metric interval in which a node's timer does not expire.

B. Performance Benchmarking

We benchmark the performance of the proposed scheme with the following approaches considered in the literature, which employ different selection schemes and selection policies.

- 1) *Window doubling-based selection scheme [17]*: In it, the $[0, 1)$ interval is divided into Z equal length intervals. If $\mu_j \in [1 - \frac{i+1}{Z}, 1 - \frac{i}{Z})$, then node j 's timer expires at $i\Delta$, for $0 \leq i \leq Z - 1$. If the first timer expiry results in a collision, then the number of intervals is doubled and the scheme is rerun. A node that was involved in the collision transmits in its respective interval with probability $\frac{1}{2}$, so as to reduce the odds of subsequent collisions. The process continues until a success occurs. The window size can be doubled up to a maximum of Z_{\max} , and remains unchanged thereafter. We set $Z = 7$ and $Z_{\max} = 1023$, as per [17]. The feedback from the sink is assumed to incur a negligible time overhead.
- 2) *Polling scheme*: In this contention-free scheme, the sink asks each of the k nodes for its metric value. This requires k slots. It then selects the best node and transmits to it.
- 3) *Threshold-based selection scheme [16]*: This scheme runs over N time slots. A node transmits in a slot with probability p if its channel gain exceeds a threshold η . Among the slots in which only node transmits, the sink chooses one slot randomly with equal probability and selects the node that transmitted in it. The parameters p and η are optimized to maximize the average data rate,

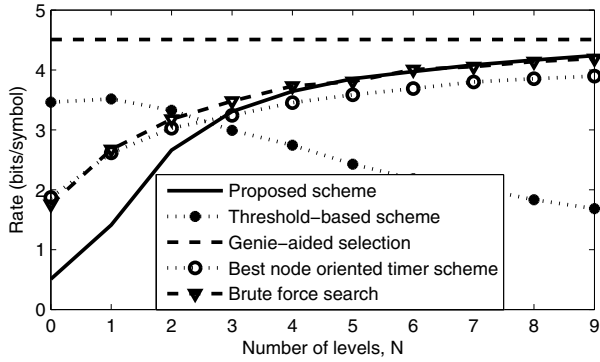


Fig. 5. Comparison of average data rate (bits/symbol) vs. N of the various schemes ($k = 10$).

as per [16].¹

- 4) *Optimized (opt.) inverse metric timer scheme* [4]: In this popular scheme, a node i sets its timer as c/μ_i . To be fair, we numerically optimize c for each setting of the system parameters and also use pragmatic selection for this scheme.
- 5) *Best node oriented timer scheme* [19]: Each node uses the metric-to-timer mapping of [19], which maximizes the probability of selecting the *best node* given T_{\max} . If the best node's timer does not expire or it collides, then an outage occurs.

We also consider *genie-aided selection*, in which the sink is assumed to select the best node always and it does so instantaneously. While this is practically impossible, it serves as an upper bound on the system performance. Rate adaptation is employed by all the above schemes.

We compare the schemes on the basis of the following two criteria: (i) *Average data rate*, which is the rate obtained in the data transmission phase that follows selection. It measures the effectiveness of a scheme in selecting nodes with higher data rates, and (ii) *Net throughput*, which accounts for the time overhead of selection. While these two criteria are equivalent for comparing schemes whose selection duration is the same, this is not so when the selection times of different schemes are different.

1) *Average Data Rate Comparisons*: Figure 5 plots the average data rate as a function of N for $k = 10$ nodes for the proposed scheme, genie-aided selection, best node oriented timer scheme, and the threshold-based scheme.² To evaluate the sub-optimality of the assumption in Sec. III-B3, which makes the normalized thresholds lie at the boundaries of the timer intervals, we also plot the average data rate achieved by a timer mapping whose interval lengths are determined using a brute force numerical search that does not use the assumption.

¹In [16], the sink is assumed to select one of the k nodes with equal probability in case none of the slots resulted in a success. However, in this case, the sink does not know the metric of the node it randomly selects, and cannot ensure reliable transmission. Furthermore, in the threshold-based and polling schemes, the node needs to feed back to the sink the rate at which it can receive data. This is not required for the proposed scheme since the time of expiry of the timer conveys this information.

²Since the duration of the selection phases of polling and window doubling-based selection cannot be preset to T_{\max} , we compare them on the basis of their net throughputs in Sec. IV-B2. The inverse timer mapping performs the worst among all the schemes, and is not shown to avoid clutter.

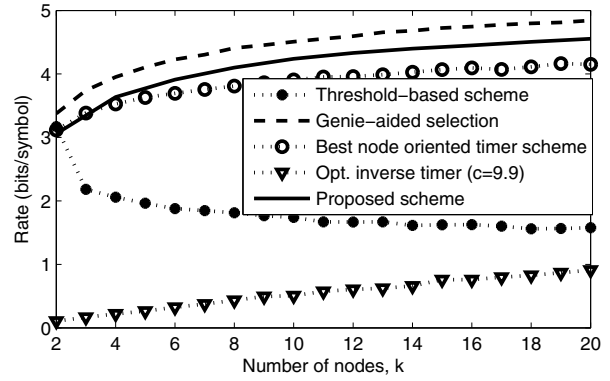


Fig. 6. Comparison of average data rate (bits/symbol) vs. number of nodes k of the various schemes ($N = 9$).

We see that the impact of this assumption is negligible even when N is as small as 4. It is also for this reason that the best node oriented timer scheme outperforms the proposed scheme for $N \leq 3$. It is also in this regime that the threshold-based scheme outperforms the proposed scheme. The average data rate of the proposed scheme rapidly approaches that of genie-aided selection as N increases, and is within 6% for $N = 9$. This is unlike the threshold-based scheme.

Figure 6 compares the average data rates as a function of the number of nodes k for $N = 9$. The proposed scheme again outperforms the benchmark schemes and is close to the genie-aided scheme. As k increases, its average data rate increases, which shows its ability to exploit multi-user diversity. Notice that the average data rate of the optimized inverse timer mapping is much lower than that of the proposed scheme, which demonstrates the importance of optimizing the timer mapping. While the best node oriented timer scheme performs almost as well as the proposed scheme for $k \leq 4$, its sub-optimality manifests itself for larger k .

2) *Net Throughput Comparisons*: The net throughput $R_{\text{eff}}(N, k)$ is given by

$$R_{\text{eff}}(N, k) = \frac{T_d \bar{R}_{N,k}}{(N+1)\Delta + T_d}, \quad (13)$$

where T_d is the duration of data transmission.

Figure 7 plots the net throughput as a function of k for $T_d = 5\Delta$. Similarly, Figure 8 plots the corresponding net throughputs for $T_d = 40\Delta$. In both figures, the proposed scheme, which is designed for $N = 4$, outperforms threshold-based scheme, window doubling-based selection, optimized inverse timer mapping scheme, and best node oriented timer scheme for $k \geq 4$. Notice that the contention-free polling scheme outperforms the proposed scheme and all the other multiple access-based for $k \leq 7$ and $k \leq 14$ for $T_d = 5\Delta$ and $T_d = 40\Delta$, respectively. However, as k increases, the throughput of the polling scheme quickly decreases. This is unlike the multiple access schemes, whose net throughput increases with k .

3) *Optimizing T_{\max}* : Having determined the optimal mapping as a function of N , we now optimize N , which is equivalent to optimizing T_{\max} , to maximize the net throughput. Intuitively, setting T_{\max} too small reduces the odds of

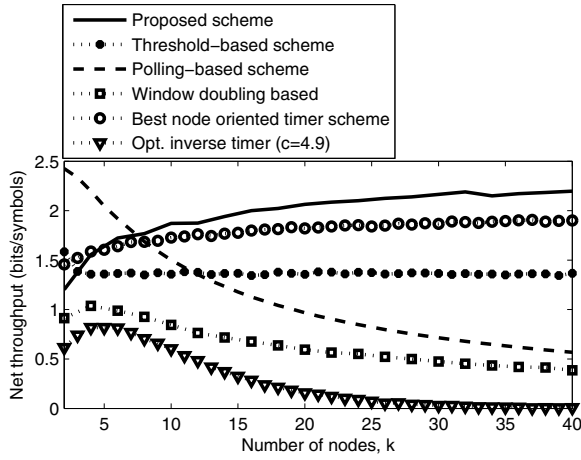


Fig. 7. Comparison of the net throughput (bits/symbol) vs. number of nodes k of the various schemes ($\frac{T_d}{\Delta} = 5$).

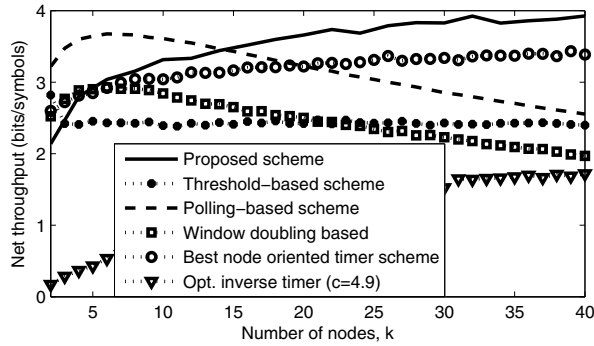


Fig. 8. Comparison of the net throughput (bits/symbol) vs. number of nodes k of the various schemes ($\frac{T_d}{\Delta} = 40$).

better nodes being selected, while setting T_{\max} too large reduces the relative time available for data transmission. Thus, there exists a trade-off between increasing the probability of selecting better nodes and increasing the time available for data transmission to the selected node.

Figure 9 plots the net throughput of the proposed scheme as a function of the number of nodes for $\frac{T_d}{\Delta} = 20$ for different N . We see that the optimal value of N , denoted by N^* , is close to 4. Table II lists N^* for different $\frac{T_d}{\Delta}$. We see that N^* increases with T_d/Δ , which occurs because the system can afford to spend more time on selection. Furthermore, $N^* \ll \frac{T_d}{\Delta}$. For asymptotically large number of nodes, N^* can be shown to be equal to the integer nearest to the solution of the following equation in N :

$$(1 - e^{-1})^{N+1} \left[1 - \left(N + 1 + \frac{T_d}{\Delta} \right) \log(1 - e^{-1}) \right] = 1. \quad (14)$$

The proof is omitted due to space constraints. From the table, we observe that the asymptotically optimal value is quite close to the optimal value for larger T_d/Δ or k . It, thus, provides a quick estimate for the optimal selection duration.

C. Individual Node Performance

To understand the impact of pragmatic selection, we plot the probability that the i^{th} best node is selected for $k = 15$

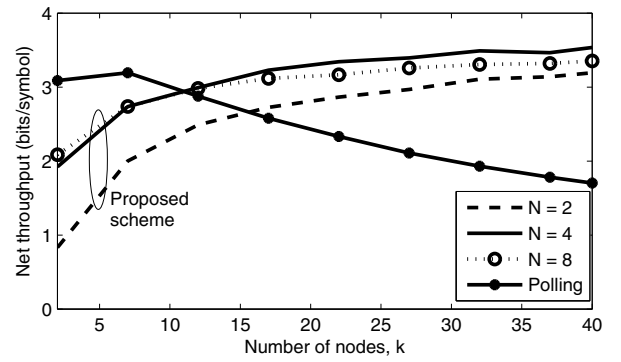


Fig. 9. Optimizing N to maximize the net throughput of the proposed scheme and comparison with the polling scheme ($\frac{T_d}{\Delta} = 20$).

TABLE II
OPTIMAL NUMBER OF TIMER LEVELS N^* THAT MAXIMIZES THE NET SYSTEM THROUGHPUT AS A FUNCTION OF k AND $\frac{T_d}{\Delta}$.

$\frac{T_d}{\Delta}$	5	20	40	60	80	100
$k = 3$	5	5	8	8	8	8
$k = 40$	2	5	6	6	8	8
$k \rightarrow \infty$	2	4	5	6	7	7

and for different values of N in Figure 10. Notice first that the probability that the second best node is selected is always zero. This is because its timer either collides with that of the best node or the best node itself gets selected. As N increases, the probability that no node is selected decreases, and the probability that the best node is selected increases. However, even for $N = 5$, the probability that a node other than the best node gets selected is 14%, which is quite significant and justifies the intuition behind pragmatic selection.

V. CONCLUSIONS

Unlike contention-free selection algorithms such as polling, which do not scale well with the number of nodes, low feedback timer-based selection algorithms are scalable, but are affected by collisions because of their distributed, multiple access nature. We saw that the selection scheme, the selection policy, and the discrete rate adaptation rule together determine the performance of an opportunistic multi-node system. These should, therefore, not be designed independently of one another. In order to compute the optimal timer mapping, we derived several structural properties about it that together made it substantially easier to find it in the space of all possible mappings. We saw that the optimal mapping differs from the many timer mappings considered in the literature. We also optimized the selection duration to maximize the net system throughput, which accounts for the time overhead of selection.

We saw that the optimal mapping outperforms all the other timer-based schemes. It also outperforms the opportunistic threshold-based multiple access scheme and polling except when the selection time or the number of nodes is very small. The increase in selection overhead of polling as the number of nodes increases impairs its ability to exploit multi-user diversity and, in fact, reduces its net throughput. An interesting avenue for future work is extending the results to the case where the metrics are not statistically identical.

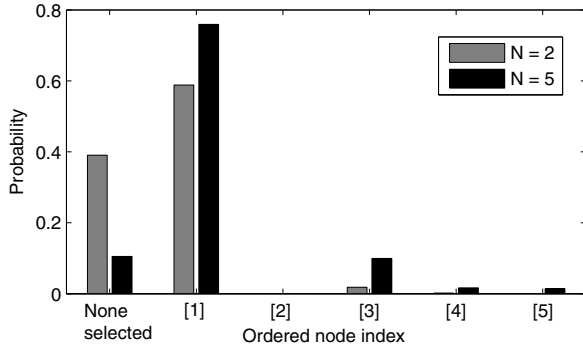


Fig. 10. Probability that the proposed scheme selects the i^{th} best node as a function of i ($k = 15$).

APPENDIX

A. Proof of Result 1

Let $f : [0, 1) \rightarrow [0, T_{\max}]$ be an MNI metric-to-timer mapping. Consider a mapping g that is defined in terms of f as follows:

$$g(\mu) = \begin{cases} f(\mu), & \mu \geq \Gamma_{M-1}^{\text{eq}}, \\ T_{\max}^+, & \text{otherwise,} \end{cases} \quad (15)$$

where T_{\max}^+ indicates that the timer does not expire before T_{\max} . Since f is MNI, it can be verified that g is well defined and MNI. We now prove for each realization of metrics that the average data rate using the mapping g is greater than or equal to that when f is used.

In a given realization $\mu_{(1)}, \dots, \mu_{(k)}$, say f selects the i^{th} best node, i.e., node (i) . The following three cases arise:

(a) $\mu_{(i)} \geq \mu_{(i+1)} > \Gamma_{M-1}^{\text{eq}}$: Since node (i) got selected, its timer did not collide with the timer of node $(i+1)$. From the definition of g , we have $g(\mu_{(j)}) = f(\mu_{(j)})$, for all $1 \leq j \leq i+1$. Hence, node (i) will again get selected by the timer mapping g . Therefore, the data rate achieved by g is the same as achieved by f .

(b) $\mu_{(i)} > \Gamma_{M-1}^{\text{eq}} \geq \mu_{(i+1)}$: In this case, $g(\mu_{(j)}) = f(\mu_{(j)})$, for all $1 \leq j \leq i$. Furthermore, the timer of node $(i+1)$ does not expire when g is used, which implies that it will not collide with the timer of node (i) when g is used. Hence, node (i) still gets selected by g , and the rate remains the same.

(c) $\Gamma_{M-1}^{\text{eq}} \geq \mu_{(i)} > \mu_{(i+1)}$: In this case, the selection of node (i) when f is used implies that the timers of nodes $(1), \dots, (i-1)$ collided when f is used. From the definition of g , we know that they will also collide when g is used. Furthermore, the timers of nodes $(i), \dots, (k)$ do not expire when g is used. Thus, no node gets selected, which implies a rate of 0. This is the same as the rate achieved when f selects node (i) since $\mu_{(i)} \leq \Gamma_{M-1}^{\text{eq}}$ implies that the rate assigned will be $R_M = 0$.

Thus, the average data rate attained by g is never less than the rate attained by f . This implies that searching only within metric-to-timer mappings that have the form of g suffices.

B. Proof of Result 2

Let $f : [0, 1) \rightarrow [0, T_{\max}]$ be an optimal MNI metric-to-timer mapping. Consider a new mapping g that is defined in

terms of f as follows:

$$g(\mu) = \begin{cases} \left\lfloor \frac{f(\mu)}{\Delta} \right\rfloor \Delta, & \text{if } f(\mu) \leq T_{\max}, \\ f(\mu), & \text{if } f(\mu) = T_{\max}^+. \end{cases} \quad (16)$$

Therefore, $g(\mu) = 0$, if $0 \leq f(\mu) < \Delta$, $g(\mu) = \Delta$, if $\Delta \leq f(\mu) < 2\Delta$, and so on. Since f is MNI, it can be easily verified that g is well-defined and MNI.

We prove below that the average data rate obtained by using g as the timer mapping is never less than that obtained by using f . Consider a given realization of metrics $\mu_{(1)}, \dots, \mu_{(k)}$. If no timer expires before T_{\max} when f is used, then the rate achieved will be zero. The definition of g in (16) implies that that no timer will expire even when g is used in this case. Thus, rates of both f and g are the same (zero).

Else, let $l \geq 1$ timers $T_{(1)}, \dots, T_{(l)}$ expire before T_{\max} for f , where $T_{(1)} = f(\mu_{(1)}), \dots, T_{(l)} = f(\mu_{(l)})$. Let node (i) , where $1 \leq i \leq l$, get selected by pragmatic selection. From (16), the corresponding timer values for g , denoted by $T'_{(1)}, \dots, T'_{(l)}$, are $T'_{(1)} = \left\lfloor \frac{T_{(1)}}{\Delta} \right\rfloor \Delta, \dots, T'_{(l)} = \left\lfloor \frac{T_{(l)}}{\Delta} \right\rfloor \Delta$. Furthermore, the timers of nodes $(l+1), \dots, (k)$ do not expire when g is used. The following three cases arise.

Case 1: $T_{(i+1)}$ also expired before T_{\max} and $i \geq 2$: Since node (i) got selected, this implies for pragmatic selection that the timers that expired at $T_{(1)}, \dots, T_{(i-1)}$ all collided with one another and timers that expired at $T_{(i-1)}$ and $T_{(i+1)}$ did not collide with $T_{(i)}$. Therefore, $T_{(i+1)} - T_{(i)} \geq \Delta$ and $T_{(i)} - T_{(i-1)} \geq \Delta$. Hence, from the definition of the floor function, we have

$$\left\lfloor \frac{T_{(i+1)}}{\Delta} \right\rfloor \geq \left\lfloor \frac{T_{(i)}}{\Delta} \right\rfloor + 1 \quad \text{and} \quad \left\lfloor \frac{T_{(i-1)}}{\Delta} \right\rfloor \leq \left\lfloor \frac{T_{(i)}}{\Delta} \right\rfloor - 1. \quad (17)$$

From (16), $T'_{(i-1)} = \left\lfloor \frac{T_{(i-1)}}{\Delta} \right\rfloor \Delta$, $T'_{(i)} = \left\lfloor \frac{T_{(i)}}{\Delta} \right\rfloor \Delta$, and $T'_{(i+1)} = \left\lfloor \frac{T_{(i+1)}}{\Delta} \right\rfloor \Delta$. Therefore, (17) implies that $T'_{(i+1)}, T'_{(i)}$, and $T'_{(i-1)}$ also do not collide with each other. Therefore, when g is used, either node (i) or one of the better nodes $(1), \dots, (i-1)$ will get selected. Thus, the rate of the node selected by g is greater than or equal to that of f .

The arguments for the following remaining two cases are along similar lines, and are not repeated to conserve space: (i) $T_{(i+1)}$ expires before T_{\max} and $i = 1$, and (ii) $T_{(i+1)}$ does not expire before T_{\max} , i.e., $T_{(i)}$ is the last timer to expire.

Thus, for every realization of metrics, the rate obtained by using g is greater than or equal to that obtained by using f . Since f is optimal by assumption, the discrete mapping must, therefore, also be optimal.³

C. Proof of Result 3

For a given realization of metrics, recall that x_i , for $0 \leq i \leq N$, denotes the number of nodes whose metrics lie in the i^{th} interval, i.e., in $[1 - \sum_{j=0}^i \alpha[j], 1 - \sum_{j=0}^{i-1} \alpha[j])$. The number of ways of placing x_0 nodes in the 0^{th} interval, x_1 nodes in

³While the first step in the proof, which is (16), is similar to that in [19], the subsequent steps and logic differ since the pragmatic selection policy may select a node other than the best node. Furthermore, our goal is to maximize average data rate, which is different from the goal in [19] of maximizing the probability that the best node is selected.

the 1st interval, ..., x_N nodes in the N^{th} interval is given by the multinomial function $\binom{k}{x_0, \dots, x_N}$.

Since the metric of a node is uniformly distributed over $[0, 1]$, the probability that it lies in the i^{th} interval (of length $\alpha[i]$) is $\alpha[i]$. Since the metrics are i.i.d., the probability of occurrence of each such placement is

$$\left[\prod_{i=0}^N (\alpha[i])^{x_i} \right] \left(1 - \sum_{l=0}^N \alpha[l] \right)^{k - \sum_{i=0}^N x_i},$$

where $\left(1 - \sum_{l=0}^N \alpha[l] \right)^{k - \sum_{i=0}^N x_i}$ is the probability that the remaining $N - \sum_{i=0}^N x_i$ nodes lie in the interval $[0, 1 - \sum_{l=0}^N \alpha[l]]$ (in which no timer expires). Furthermore, by the definition of the selection location function $\mathcal{S}(\mathbf{x})$, the rate achieved by the timer scheme is given by $\psi \left(1 - \sum_{j=0}^{\mathcal{S}(\mathbf{x})} \alpha[j] \right)$. Thus, from the law of total expectation, the average data rate is given by (5).

D. Proof of Result 4

We start with the expression for the average data rate in (5). Notice that in the right hand side (RHS) of (5), each x_j can take values only between 0 and k . We now evaluate sums of terms where $x_0 = 1$ (success in the 0th interval) and where $x_0 \neq 1$.

1) *Terms corresponding to $x_0 = 1$* : This means that the best node has successfully transmitted in the 0th interval. Hence, $\mathcal{S}(\mathbf{x}) = 0$. The summation of all the terms in (5) for which $x_0 = 1$ simplifies as follows:

$$\begin{aligned} & \sum_{\substack{\mathbf{x}=(1, x_1, \dots, x_N) \\ x_j \geq 0, \sum_{j=1}^N x_j \leq k-1}} \binom{k}{1, x_1, \dots, x_N} \left[\prod_{i=0}^N (\alpha[i])^{x_i} \right] \\ & \times \left(1 - \sum_{l=0}^N \alpha[l] \right)^{k-1 - \sum_{j=1}^N x_j} \psi \left(1 - \sum_{j=0}^{\mathcal{S}(\mathbf{x})} \alpha[j] \right) \\ & = k\alpha[0]\psi(1 - \alpha[0]) \sum_{\substack{\mathbf{x}=(x_1, \dots, x_N) \\ x_j \geq 0, \sum_{j=1}^N x_j \leq k-1}} \binom{k-1}{x_1, \dots, x_N} \\ & \times \left[\prod_{i=1}^N (\alpha[i])^{x_i} \right] \left(1 - \alpha[0] - \sum_{l=1}^N \alpha[l] \right)^{k-1 - \sum_{j=1}^N x_j}, \\ & = k\alpha[0](1 - \alpha[0])^{k-1} \psi(1 - \alpha[0]). \end{aligned} \quad (18)$$

The last step follows from the properties of multinomial expansions.

2) *Terms corresponding to $x_0 = r$, where $r \neq 1$* : This means that either no node ($r = 0$) has transmitted in the 0th interval or a collision ($r \geq 2$) has occurred in it. In either case, we see that $\mathcal{S}((x_0, x_1, \dots, x_N)) = 1 + \mathcal{S}((x_1, \dots, x_N))$. The summation A_r of the terms in (5) in which $x_0 = r$ then

simplifies as follows:

$$\begin{aligned} A_r &= \sum_{\substack{\mathbf{x}=(r, x_1, \dots, x_N) \\ x_j \geq 0, \sum_{j=1}^N x_j \leq k-r}} \binom{k}{r, x_1, \dots, x_N} \left[\prod_{i=0}^N (\alpha[i])^{x_i} \right] \\ & \times \left(1 - \sum_{l=0}^N \alpha[l] \right)^{k-r - \sum_{j=1}^N x_j} \psi \left(1 - \sum_{j=0}^{\mathcal{S}(\mathbf{x})} \alpha[j] \right), \\ & = \sum_{\substack{\mathbf{x}=(x_1, \dots, x_N) \\ x_j \geq 0, \sum_{j=1}^N x_j \leq k-r}} \binom{k}{r} \binom{k-r}{x_1, \dots, x_N} (\alpha[0])^r \left[\prod_{i=1}^N (\alpha[i])^{x_i} \right] \\ & \times \left(1 - \alpha[0] - \sum_{l=1}^N \alpha[l] \right)^{k-r - \sum_{j=1}^N x_j} \psi \left(1 - \alpha[0] - \sum_{j=1}^{\mathcal{S}(\mathbf{x})} \alpha[j] \right). \end{aligned} \quad (19)$$

Multiplying and dividing the above equation by $(1 - \alpha[0])^{k-r}$, we get

$$A_r = \binom{k}{r} (\alpha[0])^r (1 - \alpha[0])^{k-r} \overline{R}'_{N-1, k-r}, \quad (20)$$

where $\overline{R}'_{N-1, k-r}$ is given by (5). This is nothing but the average data rate obtained when the interval lengths are $\frac{\alpha[1]}{1 - \alpha[0]}, \dots, \frac{\alpha[N]}{1 - \alpha[0]}$ and the rate function is given by $\psi'(x) \triangleq \psi((1 - \alpha[0])x)$.

The two initialization equations in (7) and (8) are easily obtained by substituting $N = 0$ and $k = 1$, respectively, in (5).

E. Proof of Result 5

The expression for $\overline{R}_{N, k}$ in (5) is symmetric in $\alpha^*[0], \dots, \alpha^*[r_1 - 1]$. This is because if x_0 nodes lie in the 0th interval, x_1 nodes lie in the 1st interval, ..., x_{r_1-1} nodes lie in the $(r_1 - 1)^{\text{th}}$ interval and the data rate achieved by any of them is R_1 , then any permutation of these x_0, \dots, x_{r_1-1} elements also gives the same rate R_1 . Therefore, the optimal interval lengths $\alpha^*[0], \dots, \alpha^*[r_1 - 1]$ are equal. Similarly, we can show that (5) is symmetric in $\alpha^*[r_1], \dots, \alpha^*[r_1 + r_2 - 1]$, and so on. Hence, the result follows.

ACKNOWLEDGMENT

The authors thank Prof. Rajesh Sundaresan (IISc) for valuable inputs.

REFERENCES

- [1] S. Sesia, I. Toufik, and M. Baker, *LTE – The UMTS Long Term Evolution, From Theory to Practice*. John Wiley and Sons, 2009.
- [2] 3GPP, “High speed downlink packet access: physical layer aspects,” Tech. Rep. 25.858 v5.0.0 (2002-03), 3rd Generation Partnership Project (3GPP), 2002.
- [3] P. Viswanath, D. Tse, and R. Laroia, “Opportunistic beamforming using dumb antennas,” *IEEE Trans. Inf. Theory*, vol. 48, pp. 1277–1294, June 2002.
- [4] A. Bletsas, A. Khisti, D. P. Reed, and A. Lippman, “A simple cooperative diversity method based on network path selection,” *IEEE J. Sel. Areas Commun.*, vol. 24, pp. 659–672, Mar. 2006.
- [5] D. S. Michalopoulos and G. K. Karagiannidis, “PHY-layer fairness in amplify and forward cooperative diversity systems,” *IEEE Trans. Wireless Commun.*, vol. 7, pp. 1073–1083, Mar. 2008.

- [6] S. Yang and J.-C. Belfiore, "A novel two-relay three-slot amplify-and-forward cooperative scheme," in *Proc. 2006 Conf. Inf. Sci. Syst.*, pp. 1329–1334.
- [7] Y. Jing and H. Jafarkhani, "Single and multiple relay selection schemes and their achievable diversity orders," *IEEE Trans. Wireless Commun.*, vol. 8, pp. 1414–1423, Mar. 2009.
- [8] Q. Zhao and L. Tong, "Opportunistic carrier sensing for energy-efficient information retrieval in sensor networks," *EURASIP J. Wireless Commun. Netw.*, vol. 2005, pp. 231–241, Apr. 2005.
- [9] X. Qin and R. Berry, "Opportunistic splitting algorithms for wireless networks," in *Proc. 2004 INFOCOM*, pp. 1662–1672.
- [10] V. Shah, N. B. Mehta, and R. Yim, "Splitting algorithms for fast relay selection: generalizations, analysis, and a unified view," *IEEE Trans. Wireless Commun.*, vol. 9, pp. 1525–1535, Apr. 2010.
- [11] T. Watteyne, I. Aue-Blum, M. Dohler, and D. Barthel, "Reducing collision probability in wireless sensor network backoff-based election mechanisms," in *Proc. 2007 Globecom*, pp. 673–677.
- [12] R. Talak and N. B. Mehta, "Feedback overhead-aware, distributed, fast, and reliable selection," *IEEE Trans. Commun.*, vol. 60, pp. 3417–3428, Nov. 2013.
- [13] J. G. Choi and S. Bahk, "Cell-throughput analysis of the proportional fair scheduler in the single-cell environment," *IEEE Trans. Veh. Technol.*, vol. 56, pp. 766–778, Mar. 2007.
- [14] A. Attar, N. Devroye, H. Li, and V. C. M. Leung, "A unified scheduling framework based on virtual timers for selfish-policy shared spectrum," in *Proc. 2010 ICC*.
- [15] L. Kleinrock and F. Tobagi, "Packet switching in radio channels—part I: carrier sense multiple access modes and their throughput delay characteristics," *IEEE Trans. Commun.*, vol. 23, pp. 1400–1416, Dec. 1975.
- [16] T. Tang and R. W. Heath, "Opportunistic feedback for downlink multiuser diversity," *IEEE Commun. Lett.*, vol. 9, pp. 948–950, Oct. 2005.
- [17] C.-S. Hwang and J. M. Cioffi, "Opportunistic CSMA/CA for achieving multi-user diversity in wireless LAN," *IEEE Trans. Wireless Commun.*, vol. 8, pp. 2972–2982, June 2009.
- [18] C.-S. Hwang and J. Cioffi, "Achieving multi-user diversity gain using user-identity feedback," *IEEE Trans. Wireless Commun.*, vol. 7, pp. 2911–2916, Aug. 2008.
- [19] V. Shah, N. B. Mehta, and R. Yim, "Optimal timer based selection schemes," *IEEE Trans. Commun.*, vol. 58, pp. 1814–1823, June 2010.
- [20] R. Agarwal, C.-S. Hwang, and J. Cioffi, "Opportunistic feedback protocol for achieving sum-capacity of the MIMO broadcast channel," in *Proc. 2007 VTC – Fall*, pp. 606–610.
- [21] H. A. David and H. N. Nagaraja, *Order Statistics*, 3rd edition. Wiley Series in Probability and Statistics, 2003.
- [22] A. Papoulis, *Probability, Random Variables and Stochastic Processes*, 3rd edition. McGraw Hill, 1991.
- [23] A. Goldsmith and S.-G. Chua, "Variable-rate variable-power MQAM for fading channels," *IEEE Trans. Commun.*, pp. 1218–1230, Oct. 1997.
- [24] K. L. Baum, T. A. Kostas, P. J. Sartori, and B. K. Classon, "Performance characteristics of cellular systems with different link adaptation strategies," *IEEE Trans. Veh. Technol.*, vol. 52, pp. 1497–1507, Nov. 2003.
- [25] D. P. Bertsekas and R. G. Gallager, *Data Networks*, 2nd edition. Prentice Hall, 1992.
- [26] 3GPP, "Technical specification group radio access network; evolved universal terrestrial radio access (E-UTRA); physical layer procedures (release 8)," TS 36.213 (v8.2.0), 3rd Generation Partnership Project (3GPP), 2008.



Neelesh B. Mehta (S'98-M'01-SM'06) received his Bachelor of Technology degree in Electronics and Communications Eng. from the Indian Institute of Technology (IIT), Madras in 1996, and his M.S. and Ph.D. degrees in Electrical Eng. from the California Institute of Technology, Pasadena, CA, USA in 1997 and 2001, respectively. He is now an Associate Professor in the Dept. of Electrical Communication Eng., Indian Institute of Science (IISc), Bangalore, India. Prior to joining IISc in 2007, he was a research scientist in AT&T Laboratories, NJ, USA,

Broadcom Corp., NJ, USA, and Mitsubishi Electric Research Laboratories (MERL), MA, USA from 2001 to 2007.

His research includes work on link adaptation, multiple access protocols, cellular system design, MIMO and antenna selection, cooperative communications, energy harvesting networks, and cognitive radio. He was also actively involved in the Radio Access Network (RAN1) standardization activities in 3GPP from 2003 to 2007. He was a TPC co-chair for tracks/symposia in COMSNETS 2014, Globecom 2013, ICC 2013, SPCOM 2012, WISARD 2010 & 2011, NCC 2011, VTC 2009 (Fall), and Chinacom 2008. He has co-authored 40 IEEE transactions papers, 65+ conference papers, and three book chapters, and is a co-inventor in 20 issued US patents. He is an Editor of IEEE WIRELESS COMMUNICATIONS LETTERS and the *Journal for Communications and Networks*, and currently serves as the Director of Conference Publications on the Board of Governors of the IEEE Communications Society.



Rajat Talak (S'07) received his Bachelor of Technology degree in Electronics and Communication Engineering from the National Institute of Technology (NITK), Karnataka, India in 2010. He is currently pursuing his Master of Science degree from the Dept. of Electrical Communication Engineering, Indian Institute of Science (IISc), Bangalore, India. His current research interests include selection algorithms, cooperative communication, cellular systems, and large networks. His research inclination is towards understanding, modeling, and designing of

futuristic communication systems and networks.



Ananda T. Suresh received his Bachelor of Technology degree in Engineering Physics from Indian Institute of Technology, Madras, India in 2010. Since then he is working towards his doctorate degree at the University of California, San Diego, USA. He received his Master of Science degree in Communication Theory and Systems from the same university in 2012. His research interests lie in information theory and machine learning.